



HAL
open science

Functional definition of the tobacco protoporphyrinogen IX oxidase substrate-binding site

Ilka U Heinemann, Nina Diekmann, Ava Masoumi, Michael Koch, Albrecht Messerschmidt, Martina Jahn, Dieter Jahn

► To cite this version:

Ilka U Heinemann, Nina Diekmann, Ava Masoumi, Michael Koch, Albrecht Messerschmidt, et al.. Functional definition of the tobacco protoporphyrinogen IX oxidase substrate-binding site. *Biochemical Journal*, 2006, 402 (3), pp.575-580. 10.1042/BJ20061321 . hal-00478655

HAL Id: hal-00478655

<https://hal.science/hal-00478655>

Submitted on 30 Apr 2010

HAL is a multi-disciplinary open access archive for the deposit and dissemination of scientific research documents, whether they are published or not. The documents may come from teaching and research institutions in France or abroad, or from public or private research centers.

L'archive ouverte pluridisciplinaire **HAL**, est destinée au dépôt et à la diffusion de documents scientifiques de niveau recherche, publiés ou non, émanant des établissements d'enseignement et de recherche français ou étrangers, des laboratoires publics ou privés.

Functional definition of the tobacco protoporphyrinogen IX oxidase substrate binding site

Ilka U. Heinemann^{*}, Nina Diekmann^{*}, Ava Masoumi^{*}, Michael Koch[†], Albrecht Messerschmidt[‡], Martina Jahn^{*} & Dieter Jahn^{*1}

^{*}Institute of Microbiology, Technical University Braunschweig, Spielmannstr. 7, 38106 Braunschweig, Germany;

[†]The Division of Structural Biology, The Wellcome Trust Centre for Human Genetic, Roosevelt Drive, Headington, Oxford, OX3 7BN, U.K.

[‡]Department of Proteomics and Signal Transduction, Max Planck Institute of Biochemistry, Am Klopferspitz 18, 82152 Martinsried, Germany;

¹Address correspondence to: Telephone: +49-531-391-5801 Fax: +49-531-391-5854

URL [http:// www.tu-braunschweig.de/ifm/abt/jahn](http://www.tu-braunschweig.de/ifm/abt/jahn); E-mail address: d.jahn@tu-bs.de (Dieter Jahn)

SHORT TITLE: PPO: substrate recognition

ABSTRACT

PPO (protoporphyrinogen IX oxidase) catalyses the flavin-dependent six-electron oxidation of protogen (protoporphyrinogen IX) to form proto (protoporphyrin IX), a crucial step in heme and chlorophyll biosynthesis. The apparent K_m value for wildtype tobacco PPO2 (mitochondrial PPO) was 1.17 μM , with a v_{max} of 4.27 $\mu\text{M min}^{-1}\text{mg}^{-1}$ and a catalytic activity k_{cat} of 6.0 s^{-1} . Amino acid residues that appear important for substrate binding in a crystal structure based model of the substrate docked in the active site were interrogated by site-directed mutagenesis. PPO2 variant F392H did not reveal detectable enzyme activity indicating an important role of Phe³⁹² in substrate ring A stacking. Mutations of Leu³⁵⁶, Leu³⁷² and Arg⁹⁸ increased k_{cat} values up to 100-fold indicating that the native residues are not essential for establishing an orientation of the substrate conducive to catalysis. Increased K_m values of these PPO2 variants from 2 - 100-fold suggest that these residues are involved but not essential to substrate binding via ring B and C. Moreover, one prominent structural constellation of human PPO causing the disease variegate porphyria (N67W/S374D) was successfully transferred into the tobacco PPO2 background. Therefore, tobacco PPO2 represents a useful model system for the understanding of the structure-function relationship underlying detrimental human enzyme defects.

KEY WORDS

Heme biosynthesis, Protoporphyrin, Mutant variants, Variegate Porphyria, Enzyme Kinetics, Stopped-Flow Fluorescence

ABBREVIATIONS

PPO, protoporphyrinogen IX oxidase; PPO2, mitochondrial protoporphyrinogen IX oxidase; protogen, protoporphyrinogen IX; proto, protoporphyrin IX; VP, Variegate Porphyria; PPO1, plastidic protoporphyrinogen IX oxidase; INH, 4-bromo-3-(5'-carboxy-4'-chloro-2'-fluoro-pheny)-1-methyl-5-trifluoromethyl-pyrazol.

INTRODUCTION

PPO (protoporphyrinogen IX oxidase, EC 1.3.3.4) catalyses the oxygen-dependent aromatisation of protogen (protoporphyrinogen IX) to proto (protoporphyrin IX) [1] (Fig. 1). It is the last common step of tetrapyrrole biosynthesis for the formation of hemes and chlorophylls. Initially, the enzyme was characterised from yeast [2] and mammalian liver [3, 4]. It catalyses the six-electron oxidation of protogen using a flavin cofactor and molecular oxygen as terminal electron acceptor. PPO is described as soluble monomer in *Bacillus subtilis* [5], as membrane-associated monomer in bovine [6] or as homodimer in *Myxococcus xanthus* and humans [7-9]. In eukaryotes PPO is associated with the outer surface of the inner mitochondrial membrane [10], while the plant enzyme is additionally located in chloroplasts [11, 12].

In humans, partial PPO deficiency causes a disease known as VP (variegate porphyria, OMINTM accession number 176200) that is inherited as an autosomal dominant trait displaying incomplete penetrance [13]. The biochemical abnormalities found in VP patients include overproduction and increased excretion of porphyrins and porphyrin precursors. VP manifests clinically with photosensitivity and acute attacks, which includes various neuropsychiatric symptoms [14]. In South Africa VP is common due to a founder effect, where mainly one amino acid exchange from Arg⁵⁹ to tryptophan causes the disease [15-18]. However, there are various additional mutations known to cause VP [19].

In plants two isoforms of PPO, PPO1 (plastidic PPO) and PPO2 (mitochondrial PPO) have been found [11, 20, 21]. They share an amino acid sequence identity of less than 30%. Both enzymes operate as homodimers and use FAD as cofactor. Recently, the crystal structure of tobacco (*Nicotiana tabacum*) PPO2 with the bound inhibitor INH (4-bromo-3-(5'-carboxy-4'-chloro-2'-fluoro-pheny)-1-methyl-5-trifluoromethyl-pyrazol) and non-covalently bound FAD has been solved [22]. This crystal structure is the only currently available structural information for eukaryotic PPO at the atomic level.

The structure of tobacco PPO2 revealed a loosely associated dimer, each monomer consisting of a membrane-, an FAD- and a substrate-binding domain, respectively. The inhibitor INH was found to be located in the active-site domain and consists of a phenyl- and pyrazol-ringsystem. Even though the FAD is not covalently bound to the enzyme it was found in close proximity to the cocrystallized inhibitor in the active site cavity. A potential reaction mechanism was proposed based on the fact that the substrate has only limited space to rotate in the active site. The six electron oxidation of proto to proto is supposedly catalysed via three steps. Three times the FAD cofactor is reduced by two electrons from the tetrapyrrole ring and reoxidised by molecular oxygen which in turn is reduced to H₂O₂. The reduction starts at the C₂₀ atom of the tetrapyrrole via enamine-imine-tautomerisation and H-rearrangements [23].

Using a model calculated based on the solved crystal structure of tobacco PPO2, we have generated 14 variant proteins carrying amino acid residue exchanges in the corresponding positions of the active-site domain. The mutant variant proteins were kinetically characterised by steady state and stopped-flow fluorescence spectrometry. Furthermore, the amino acid residues responsible for the most common cause of VP in humans were replaced and analysed on the basis of the crystal structure of PPO2 from tobacco.

EXPERIMENTAL

Materials:

Proto was purchased from Sigma–Aldrich (Hamburg, Germany). Tween 20 was obtained from Carl Roth GmbH (Karlsruhe, Germany). The remaining chemicals were purchased from Sigma-Aldrich unless specified otherwise. Mutagenesis experiments were performed using the QuikChange™ site-directed mutagenesis kit (Stratagene, Heidelberg, Germany). Oligonucleotides were purchased from Biomers.net GmbH (Ulm, Germany). S•Tag Rapid Assay Kit was from Novagen (Darmstadt, Germany). Cells were disrupted using a sonotrode from Bandelin (Berlin, Germany). Protino® Ni-IDA Resin was from Machery-Nagel (Düren, Germany).

Site-directed mutagenesis of tobacco PPO2 gene

The *N. tabacum* PPO2 gene expression vector pET32a-PPO2(M1-K224Q) was described before [22]. The plasmid was used as template for site-directed mutagenesis. Primers to generate N67R, N67W, R98A, R98E, R98K, L356N, L356V, L372N, L372V, S374D, F392E, and F392H, respectively, were as follows:

N67R 5'-GGGATGAAGGGGCACGTACTATGACTG-3' and 5'-CAGTCATAGTACTTGCCC-TTCATCCC-3'; N67W 5'-GGGATGAAGGGGCATGGACTATGACTG-3' and 5'-CAGTCATAGTCCATGCCCCTTCATCCC-3'; R98A 5'-CCACTTTCACAAAACAAGGCCTACATTGCCAG-

AAATGG-3' and 5'-CCATTTCTGGCAATGTAGGCCTTGTTTTGTGAAAGTGG-3'; R98E 5'-CCACTTTCACAAAACAAGGAGTACATTGCCAGAAATGG-3' and 5'-ATTTCTGGCAATGTACTCCTTGTT-TTGTGAAAGTGG-3'; R98K: 5'-CCACTTTCACAAAACAAGAAGTACATTGCCAGAAATGG-3' and 5'-CCATTTCTGGCAATGACTTTGTTGTGAAAGTGG-3'; L356N 5'-GGTGGGGTTAATGTACCTTCCAAGGAGC-3' and 5'-GCTCCTTGGAAAGTACA-TTACCCAAAGCCC-3'; L356V 5'-GGGCTTTGGGGTTGTTGTACCTTCCAAGGAGC-3' and 5'-GCTCCTTGGAAAGTACAACAACCCCAAAGCCC-3'; L372N 5'-GACTAGGCACCAACTTCTCTTCTATGATGTTTCC-3' and 5'-GGAAACATCATAGAAGAGAAGTTGGTGCCTA-GTGTC-3'; L372V 5'-GACTAGGCACCGTCTTCTCTTCTATGATGTTTCC-3' and 5'-GGAAACATCATAGAAGAGAAGACGGTGCCTAGTGTC-3'; S374D 5'-GACTAGGCACCCTCTTCGATTCTATGATGTTTCC-3' and 5'-GGAAACATCATAGAATCGAAGAGGGTGCC-TAGTGTC-3'; F392E 5'-CTCTATACTACTGAGGTTGGTGGAAAGCC-3' and 5'-GGCTTCCA-CCAACCTCAGTAGTATAGAG-3'; F392H 5'-CTCTATACTACTCATGTTGGTGGAAAGCC-3' and 5'-GGCTTCCACCAACATGAGTAGTATAGAG-3. Individual mutations were combined to generate the double-mutation carrying variants N67R/S374D and N67W/S374D, respectively. For all introduced mutations overall PPO2 gene integrity was verified by DNA sequence determination.

Recombinant production and purification of *N. tabacum* PPO2 and its variants

Recombinant proteins were produced using *E. coli* strain BL21(DE3)RIL (Stratagene, Heidelberg, Germany) containing the original or mutated pET32a-PPO2-plasmids. Cells were grown in LB medium at 37 °C under vigorous aeration. When the cultures reached an absorbance at λ_{578} of 0.7 protein production was induced by the addition of 250 μ M isopropyl-1-thio- β -D galacto-pyranoside. Cells were further cultivated overnight at 25 °C, 150 rpm, harvested, washed with buffer A (10 mM Tris HCl pH 8.0, 300 mM NaCl, 10 mM MgCl₂, 0.05 % Triton X-100) and resuspended in a minimal volume of buffer A. Cells were broken by sonication (Bandelin HD 2070, 0.5 sec sound, 0.5 sec paused, MS73 tip, 70 % amplitude) and the cell free extract cleared by centrifugation at 175.000 g for 45 min. Protein integrity was verified via Western blot analysis. Recombinant PPO2 were purified to apparent homogeneity by Protino[®] Ni-IDA Resin (Machery-Nagel, Düren, Germany) as outlined in the manufacturers instructions. PPO concentrations were determined via S•Tag Rapid Assay Kit. Protein purification and integrity were analyzed by mass spectrometry and SDS-polyacrylamide gel electrophoresis as outlined before [24]. The overall protein folding was analyzed by CD spectroscopy using a Jasco J810 CD spectropolarimeter as described before [25, 26]. The flavin content of each mutant enzyme was determined spectroscopically as outlined before and is given in table 1 [9, 27].

PPO assays

The substrate protogen was produced as described before [28, 29]. PPO2 activity was monitored using a continuous assay via the detection of proto fluorescence. Stopped-flow kinetic experiments were performed under aerobic conditions using a Jasco 810 stopped-flow spectrometer and obtained data were analysed with Biokine Acquire Kinetics (Jasco, Überlingen, Germany). Averages of three to five individual transients were analysed. Protogen was dissolved in 50 mM Mes-buffer pH 6.0, 1 % (v/v) Triton X-100, 20 mM EDTA. Protogen solution and PPO2 preparations were mixed in a six to one ratio in a total volume of 300 μ l and fluorescence resulting from proto formation was continuously recorded via an excitation at 409 nm and emission measurement above 450 nm. Approximately 8000 measurement points per assay were recorded. Proto concentrations were calculated using an appropriate calibration curve. The percentage of substrate consumed was less than 5%.

Determination of kinetic constants

The Michaelis Menten constant (K_m), the maximal velocity v_{max} and the catalytic constant k_{cat} were determined from substrate velocity plots by measuring the constant velocity formation of proto from protogen over a substrate range from 1 - 25 μ M and a time course of up to 2 hours at 20°C. The initial reaction rates were linear and values were determined by the computerised Lineweaver Burke iterative curve fitting using SigmaPlot 8.0 Enzyme Kinetics v1.1. For the calculation of the catalytic efficiency k_{cat} , the maximal velocity v_{max} was divided by the corresponding enzyme concentration.

RESULTS AND DISCUSSION

Active site architecture of *N. tabacum* PPO2.

The crystal structure of tobacco PPO2 revealed a close insight into the three-dimensional structure of the enzyme [22]. Modelling of the protogen into the active site of tobacco PPO2 is based on the first model proposed by Koch *et al.* [22]. Residues Arg⁹⁸, Phe³⁹², Leu³⁷² and Leu³⁵⁶ coordinated the inhibitor INH which was co-crystallised within the active site of PPO2. These four amino acid residues were found highly conserved throughout the PPO family. Ring A is coordinated via aromatic stacking with Phe³⁹² (Fig. 2 A) [22]. The side chains of Leu³⁵⁶ and Leu³⁷² interact hydrophobically with ring B. The side chain of residue Arg⁹⁸ forms a salt bridge to the propionate carboxyl group of ring C. Additionally ring C might be stabilised by flipping and subsequent stacking of the conserved residue Phe³⁵³. The dome conformation of the protogen is probably stabilised by the carbonyl oxygen of the highly conserved Gly¹⁷⁵.

Experimental determination of amino acid residues important for substrate binding

Based on the proposed model we functionally investigated the molecular basis of substrate coordination and its catalytic implications. We constructed an appropriate set of mutant PPO2 genes, isolated the respective mutant protein variants and determined their kinetic parameters via fluorescence stopped flow spectrometry in comparison to wildtype PPO2. We used the strategy of introducing conservative and non-conservative amino acid exchanges for residues of interest in order to evaluate their chemical contribution to substrate binding and catalysis. Obtained results are listed in table 1. The apparent K_m value of purified wildtype PPO2 protein for its substrate was 1.17 μM with a k_{cat} value of 6.0 s^{-1} . The determined kinetic parameters were within the range of values measured for PPOs from other organisms, e.g. $K_m = 1.0 \mu\text{M}$, $k_{\text{cat}} = 0.0031 \text{s}^{-1}$ for *B. subtilis* [30], $K_m = 0.1 \mu\text{M}$ for *Saccharomyces cerevisiae* [31], $K_m = 2.8 \mu\text{M}$ for *Aquifex aeolicus*, [32] and $K_m = 0.85 \mu\text{M}$ and for *Homo sapiens* either a $k_{\text{cat}} = 0.175 \text{s}^{-1}$ [7] or a $k_{\text{cat}} = 5.95 \text{s}^{-1}$ [9], respectively. The FAD content of PPO2 was 0.63 moles FAD/subunit PPO2. All PPO2 mutant enzymes revealed a similar FAD content, the only exception being the double mutant N67W/S374D which is discussed in detail later (table 1).

The crystal structure revealed that ring A of the inhibitor INH is kept in position by aromatic stacking with residue **Phe**³⁹², which during reaction stabilises the electron transfer over the ring. An amino acid exchange to Glu³⁹² in the variant F392E was tolerated within the active site cavity and resulted in inferior binding of the substrate protogen ($K_m = 11.2 \mu\text{M}$). However, once the substrate protogen was bound, its conversion was catalysed sufficiently ($k_{\text{cat}} = 11 \text{s}^{-1}$). The tetrapyrrole ring is made positive by the hydride abstraction at the N5 atom of FAD. Thus the negative charge of the introduced glutamate might stabilise the ring and catalysis may proceed equally fast. In this case only the stabilisation of the substrate by aromaticity is lowered and so its binding is weaker. Additionally, the PPO2 variant F392H was found to be virtually inactive. Determination of reliable kinetic parameters was not possible. Histidine at a pH below its pK at 6.1 is positively charged. Here at a pH of 6.0, this holds true for most histidine molecules of PPO2. The positive charge of the histidine ring at this position lead to repulsion and obstructs substrate binding, consequently reactions kinetics collapsed (Fig. 2 A). For detailed kinetic parameters of the mutant proteins please consult table 1.

In the model for substrate binding deduced from the PPO2-INH crystal structure ring B of protogen is sandwiched between the conserved residues **Leu**³⁵⁶ and **Leu**³⁷². Both amino acid residues were exchanged to either valine or asparagine, respectively. In both cases the conservative amino acid exchange to valine enhanced catalysis up to 100-fold ($k_{\text{cat}} = 300 \text{s}^{-1}$ and $k_{\text{cat}} = 597 \text{s}^{-1}$, respectively). However, in the case of an amino acid exchange of Leu³⁷² to valine binding of the substrate protogen was 100-fold reduced ($K_m = 103 \mu\text{M}$). In contrast to that the PPO2 variants L356N and L372N showed an only slightly inferior binding capacity compared to the wildtype and revealed comparable catalytic PPO2 activities (see table 1). Valine possesses comparable hydrophobic features to leucine. However,

the carbon backbone of the side chain is shorter than that of leucine. Most likely the appropriate location of the hydrophobic residue in relation to the coordinated substrate ring is essential, explaining the increasing K_m values of L356V and especially L372V. Once the substrate is bound catalysis is found enhanced for both mutants. Most likely the smaller side chain of valine better accommodates the necessary complex arrangement of the substrate during catalysis. On the other hand asparagine obviously provides the necessary side-chain length and chemical character to supplement for leucine in both positions (Fig. 2A). The next investigated amino acid residue potentially involved in substrate binding was **Arg⁹⁸**. It was deduced from the *N. tabacum* PPO2 crystal structure that Arg⁹⁸ provides the counter charge for the carboxylate group of the inhibitor which most likely mimics the propionate group of ring C of protogen. The PPO2 variants R98K, R98E and R98A were chosen to evaluate the contribution of this positively charged amino acid. While the conservative exchange R98K improved enzyme activity ($k_{cat} = 37 \text{ s}^{-1}$), the non-conservative exchange R98E resulted in inferior substrate binding ($K_m = 12.5 \text{ }\mu\text{M}$). Most likely the introduced negative charge prohibited the ionic interaction necessary for the stabilisation of ring C. In agreement with this assumption the replacement of Arg⁹⁸ with the non polar amino acid alanine resulted in an enzyme variant (R98A) with an eight-fold increased K_m value (Fig. 2 A). Interestingly, all three variants in position 98 showed an increased k_{cat} value, especially variant R98A ($k_{cat} = 309 \text{ s}^{-1}$), indicating improved turnover in the absence of ionic interaction between enzyme and substrate. Nevertheless the overall response of PPO2 towards the introduced amino acid exchanges in position 98 is nicely reflected by the k_{cat} and K_m values.

In summary, by measuring enzyme activity of mutant PPO2s we were able to verify that the well conserved residues Arg⁹⁸, Phe³⁹², Leu³⁵⁶ and Leu³⁷² are functionally involved in substrate coordination within the active site.

Variegate Porphyria

The dominantly inherited genetic disorder VP in humans results from impaired PPO activity as a consequence of an amino acid residue exchange. In more than 94% of the VP cases in South Africa, Arg⁵⁹ is mutated to tryptophan [16]. The corresponding residue to human Arg⁵⁹ in the tobacco PPO2 is **Asn⁶⁷**. It is positioned on a longer loop between a β -strand and an α -helix exactly between the FAD-binding and substrate-binding sites (Fig. 2 B). The residue is conserved in all known mitochondrial and plastidic plant PPO amino acid sequences. We started to mimic the situation of the human enzyme on the basis of the related crystal structure of PPO2 from tobacco by mutating Asn⁶⁷ to arginine. The obtained mutant N67R was found to be reasonably active. Even though the mutation resulted in inferior substrate binding, the catalytic efficiency was acceptable. This observation is in agreement with the findings of Maneli *et al.* [9] who underlined the importance of a hydrophilic, favourably positively charged amino acid at position R59 in the human enzyme. Replacing Asn⁶⁷ by tryptophan

abolished enzyme activity. The bulky nature of an aromatic tryptophan in position N67 results in impaired enzyme activity. Thus, the enzymatic defect responsible for most VP cases in humans can be transferred onto tobacco PPO2. The spatial structure of PPO2 from tobacco can be used as a model for human PPO. However, in the tobacco PPO2 crystal structure the residue opposite to Asn⁶⁷ is Ser³⁷⁴ (Fig. 2 B). The corresponding residue in human PPO is Asp³⁴⁹ conserved in all known animal PPOs. Asp³⁴⁹ is likely to form a salt bridge with Arg⁵⁹, which would sterically fit in this area of the protein [22]. In order to further adapt tobacco PPO2 towards the human counterpart, we first mutated Ser³⁷⁴ to aspartate. The S374D single mutant showed reduced substrate binding capacity with a significantly increased k_{cat} value ($k_{\text{cat}} = 208 \text{ s}^{-1}$). Subsequently, we mutated Asn⁶⁷ of S374D to arginine to reconstruct the assumed salt bridge Asp³⁷⁴/Arg⁶⁷ in the human enzyme for our tobacco VP model. The resulting N67R/S374D double mutant showed an almost wildtype level K_{m} value ($K_{\text{m}} = 1.4$). We were able to obtain a PPO2 variant with wildtype like substrate recognition and even improved catalytic properties ($k_{\text{cat}} = 111 \text{ s}^{-1}$) by a reconstruction of the salt bridge in the tobacco enzyme. These results argue for the existence of a salt bridge linking Arg⁵⁹ and Asp³⁴⁹ in the human enzyme as well. The double mutation N67W/S374D, mimicking VP in the human enzyme significantly reduced enzyme activity. The K_{m} value was increased by a factor of 20 while the $k_{\text{cat}}/K_{\text{m}}$ value decreased 10 fold. Obviously the also reduced FAD content of 0.38 moles FAD/subunit for PPO2 variant N67W/S473D representing approximately 60 % of the wildtype enzyme content does not account for the observed decrease in enzyme activity. Similar observations were made for the human R59W mutant enzyme before [9]. Most importantly, in contrast to most other generated mutant enzymes this PPO2 variant showed an increased K_{m} with a parallel decreased k_{cat} compared to the double mutant N67R/S374D. Both amino acids neighbouring Asp³⁴⁹ (Ser³⁷⁴ in PPO2) in the human enzyme have previously been characterised. A mutation of tryptophan in position 348 of the human enzyme to cysteine resulted in a wildtype-like K_{m} value and a tenfold reduced k_{cat} [9]. A mutation of Ser³⁵⁰ to proline abolished enzyme activity [18]. These observations underscore that the structural integrity of this region is important for enzyme activity.

Consequently, generated mutant tobacco PPO2 enzymes, the single as well as the double mutants, may serve as a model for further investigations towards the structural understanding of the disease causing situation in the human PPO.

SUMMARY AND OUTLOOK

We conclude from our investigation that most likely all four rings of the protogen substrate of PPO2 are being coordinated during substrate binding by tobacco PPO2. Ring A is stacked by Phe³⁹², ring B is sandwiched in between Leu³⁵⁶ and Leu³⁷² and the propionate carboxylate of ring C is bound to Arg⁹⁸. Furthermore, ring D might be stacked against the A ring of the isoalloxazine moiety of the

FAD. Most of the generated PPO2 variants were characterised by an increase in K_m and K_{cat} values. One may conclude that tobacco PPO2 was optimised during evolution towards a stringent substrate recognition and discrimination and not towards catalytic turnover.

The results obtained for the VP type enzyme variants showed that the enzymatic defect responsible for causing variegate porphyria in humans can be mimicked with the tobacco PPO2 model.

ACKNOWLEDGEMENTS

This work was supported by the *Deutsche Forschungsgemeinschaft* (JA 470-7-3).

REFERENCES

- 1 Brenner, D. A. and Bloomer, J. R. (1980) The enzymatic defect in variegate porphyria. Studies with human cultured skin fibroblasts. *N. Engl. J. Med.* **302**, 765-769
- 2 Poulson, R. and Polglase, W. J. (1975) The enzymic conversion of protoporphyrinogen IX to protoporphyrin IX. Protoporphyrinogen oxidase activity in mitochondrial extracts of *Saccharomyces cerevisiae*. *J. Biol. Chem.* **250**, 1269-1274
- 3 Poulson, R. (1976) The enzymic conversion of protoporphyrinogen IX to protoporphyrin IX in mammalian mitochondria. *J. Biol. Chem.* **251**, 3730-3733
- 4 Dailey, H. A. and Karr, S. W. (1987) Purification and characterization of murine protoporphyrinogen oxidase. *Biochemistry* **26**, 2697-2701
- 5 Hansson, M. and Hederstedt, L. (1992) Cloning and characterization of the *Bacillus subtilis* hemEHY gene cluster, which encodes protoheme IX biosynthetic enzymes. *J. Bacteriol.* **174**, 8081-8093
- 6 Siepkner, L. J., Ford, M., de Kock, R. and Kramer, S. (1987) Purification of bovine protoporphyrinogen oxidase: immunological cross-reactivity and structural relationship to ferrochelatase. *Biochim. Biophys. Acta* **913**, 349-358
- 7 Dailey, T. A. and Dailey, H. A. (1996) Human protoporphyrinogen oxidase: expression, purification, and characterization of the cloned enzyme. *Protein Sci.* **5**, 98-105
- 8 Dailey, T. A. and Dailey, H. A. (1997) Expression, purification, and characteristics of mammalian protoporphyrinogen oxidase. *Methods Enzymol.* **281**, 340-349
- 9 Maneli, M. H., Corrigan, A. V., Klump, H. H., Davids, L. M., Kirsch, R. E. and Meissner, P. N. (2003) Kinetic and physical characterisation of recombinant wild-type and mutant human protoporphyrinogen oxidases. *Biochim. Biophys. Acta* **1650**, 10-21
- 10 Deybach, J. C., da Silva, V., Grandchamp, B. and Nordmann, Y. (1985) The mitochondrial location of protoporphyrinogen oxidase. *Eur. J. Biochem.* **149**, 431-435
- 11 Jacobs, J. M. and Jacobs, N. J. (1984) Protoporphyrinogen oxidation, an enzymatic step in heme and chlorophyll synthesis: partial characterization of the reaction in plant organelles and comparison with mammalian and bacterial systems. *Arch. Biochem. Biophys.* **229**, 312-319
- 12 Dailey, H. A. (2002) Terminal steps of haem biosynthesis. *Biochem. Soc. Trans.* **30**, 590-595

- 13 Kappas, A. S., S. Galbraith, R.A.; Nordmann, Y. (1995) *The Metabolic and Molecular Basis of Inherited Diseases*. McGraw-Hill, New York
- 14 Mustajoki, P. (1980) Variegate porphyria. Twelve years' experience in Finland. *Q. J. Med.* **49**, 191-203
- 15 Dean, G. (1971) Screening tests for porphyria. *Lancet*. **1**, 86-87
- 16 Meissner, P. N., Dailey, T. A., Hift, R. J., Ziman, M., Corrigall, A. V., Roberts, A. G., Meissner, D. M., Kirsch, R. E. and Dailey, H. A. (1996) A R59W mutation in human protoporphyrinogen oxidase results in decreased enzyme activity and is prevalent in South Africans with variegate porphyria. *Nat. Genet.* **13**, 95-97
- 17 Warnich, L., Kotze, M. J., Groenewald, I. M., Groenewald, J. Z., van Brakel, M. G., van Heerden, C. J., de Villiers, J. N., van de Ven, W. J., Schoenmakers, E. F., Taketani, S. and Retief, A. E. (1996) Identification of three mutations and associated haplotypes in the protoporphyrinogen oxidase gene in South African families with variegate porphyria. *Hum. Mol. Genet.* **5**, 981-984
- 18 Roberts, A. G., Puy, H., Dailey, T. A., Morgan, R. R., Whatley, S. D., Dailey, H. A., Martasek, P., Nordmann, Y., Deybach, J. C. and Elder, G. H. (1998) Molecular characterization of homozygous variegate porphyria. *Hum. Mol. Genet.* **7**, 1921-1925
- 19 von und zu Fraunberg, M., Timonen, K., Mustajoki, P. and Kauppinen, R. (2002) Clinical and biochemical characteristics and genotype-phenotype correlation in Finnish variegate porphyria patients. *Eur. J. Hum. Genet.* **10**, 649-657
- 20 Lermontova, I., Kruse, E., Mock, H. P. and Grimm, B. (1997) Cloning and characterization of a plastidal and a mitochondrial isoform of tobacco protoporphyrinogen IX oxidase. *Proc. Natl. Acad. Sci. U S A* **94**, 8895-8900
- 21 Beale, S. I. (1999) Enzymes of Chlorophyll biosynthesis. *Photosynthesis Research* **60**, 43-73
- 22 Koch, M., Breithaupt, C., Kiefersauer, R., Freigang, J., Huber, R. and Messerschmidt, A. (2004) Crystal structure of protoporphyrinogen IX oxidase: a key enzyme in haem and chlorophyll biosynthesis. *EMBO J.* **23**, 1720-1728
- 23 Phillips, J. D., Whitby, F. G., Kushner, J. P. and Hill, C. P. (2003) Structural basis for tetrapyrrole coordination by uroporphyrinogen decarboxylase. *EMBO J.* **22**, 6225-6233

- 24 Breckau, D., Mahlitz, E., Sauerwald, A., Layer, G. and Jahn, D. (2003) Oxygen-dependent coproporphyrinogen III oxidase (HemF) from *Escherichia coli* is stimulated by manganese. *J. Biol. Chem.* **278**, 46625-46631
- 25 Layer, G., Grage, K., Teschner, T., Schunemann, V., Breckau, D., Masoumi, A., Jahn, M., Heathcote, P., Trautwein, A. X. and Jahn, D. (2005) Radical S-adenosylmethionine enzyme coproporphyrinogen III oxidase HemN: functional features of the [4Fe-4S] cluster and the two bound S-adenosyl-L-methionines. *J. Biol. Chem.* **280**, 29038-29046
- 26 Randau, L., Schauer, S., Ambrogelly, A., Salazar, J. C., Moser, J., Sekine, S., Yokoyama, S., Soll, D. and Jahn, D. (2004) tRNA recognition by glutamyl-tRNA reductase. *J. Biol. Chem.* **279**, 34931-34937
- 27 Ohno, Y., Buescher, E. S., Roberts, R., Metcalf, J. A. and Gallin, J. I. (1986) Reevaluation of cytochrome b and flavin adenine dinucleotide in neutrophils from patients with chronic granulomatous disease and description of a family with probable autosomal recessive inheritance of cytochrome b deficiency. *Blood* **67**, 1132-1138
- 28 Labbe, P., Camadro, J. M. and Chambon, H. (1985) Fluorometric assays for coproporphyrinogen oxidase and protoporphyrinogen oxidase. *Anal. Biochem.* **149**, 248-260
- 29 Layer, G., Moser, J., Heinz, D. W., Jahn, D. and Schubert, W. D. (2003) Crystal structure of coproporphyrinogen III oxidase reveals cofactor geometry of Radical SAM enzymes. *EMBO J.* **22**, 6214-6224
- 30 Corrigall, A. V., Siziba, K. B., Maneli, M. H., Shephard, E. G., Ziman, M., Dailey, T. A., Dailey, H. A., Kirsch, R. E. and Meissner, P. N. (1998) Purification of and kinetic studies on a cloned protoporphyrinogen oxidase from the aerobic bacterium *Bacillus subtilis*. *Arch. Biochem. Biophys.* **358**, 251-256
- 31 Camadro, J. M., Thome, F., Brouillet, N. and Labbe, P. (1994) Purification and properties of protoporphyrinogen oxidase from the yeast *Saccharomyces cerevisiae*. Mitochondrial location and evidence for a precursor form of the protein. *J. Biol. Chem.* **269**, 32085-32091
- 32 Wang, K. F., Dailey, T. A. and Dailey, H. A. (2001) Expression and characterization of the terminal heme synthetic enzymes from the hyperthermophile *Aquifex aeolicus*. *FEMS Microbiol. Lett.* **202**, 115-119

TABLES

Table 1: Kinetic parameters of wildtype and mutant PPO2. The Michaelis Menten constant K_m , the k_{cat} and the k_{cat}/K_m values for the *N. tabacum* PPO2 were determined from substrate velocity plots by measuring the constant velocity formation of proto from protogen over the substrate range from 1-25 μM . Values were determined by the computerised Lineveaver Burk iterative curve fitting (SigmaPlot 8.0 Enzyme Kinetics v1.1). The FAD content of wildtype and mutant PPO2 were determined spectroscopically. The FAD content was calculated using standard FAD (Sigma). The standard error of the shown results was between 5 and 10 %.

Protein variant	K_m [μM] ^a	k_{cat} [s^{-1}] ^a	k_{cat}/K_m [$\mu\text{M}^{-1}\text{s}^{-1}$] ^a	FAD content [mol/mol of subunit]
Wildtype	1.17	6	5.1	0.63
Substrate binding ring A				
F392H	n.d. ^b	n.d. ^b	n.d. ^b	0.58
F392E	11.20	11	1.0	0.60
Substrate binding ring B				
L356N	11.0	38	3.4	0.55
L356V	7.30	300	41.1	0.62
L372N	16.40	7	0.4	0.60
L372V	103	597	5.8	0.53
Substrate binding ring C				
R98K	2.6	37	14.4	0.50
R98E	12.50	34	2.7	0.51
R98A	8.30	365	44	0.57
Variegate porphyria				
S374D	10.9	208	18.5	0.55
N67R	97	97	1.0	0.61
N67W	n.d. ^b	n.d. ^b	n.d. ^b	0.48
N67R/S374D („human PPO“)	1.4	111	79.4	0.65
N67W/S374D („human VP“)	21	12	0.57	0.38

^a Determination of kinetic constants was performed as described under “Experimental”

^b Not detectable

FIGURE LEGENDS

Fig. 1: Reaction scheme of PPO.

Protopogen is oxidised to proto by molecular oxygen with the generation of hydrogen peroxide. Hydrogen atoms eliminated during the reaction are written in bold letters.

Fig. 2: Active site cavity of PPO2.

(A) Active site of tobacco PPO2. Depicted are the investigated Arg⁹⁸, Leu³⁵⁶, Leu³⁷² and Phe³⁹². Residue Phe³⁹² is shown to coordinate ring A of the protogen. Leu³⁵⁶ and Leu³⁷² are stacking protogen ring B from the “back” and the “front”, Arg⁹⁸ is supposed to coordinate the propionate carboxylate group of the protogen ring C, respectively. (B) Variegate Porphyria mutants of tobacco PPO2. Residues Asn⁶⁷ and Ser³⁷⁴ playing an important role in human VP are depicted.

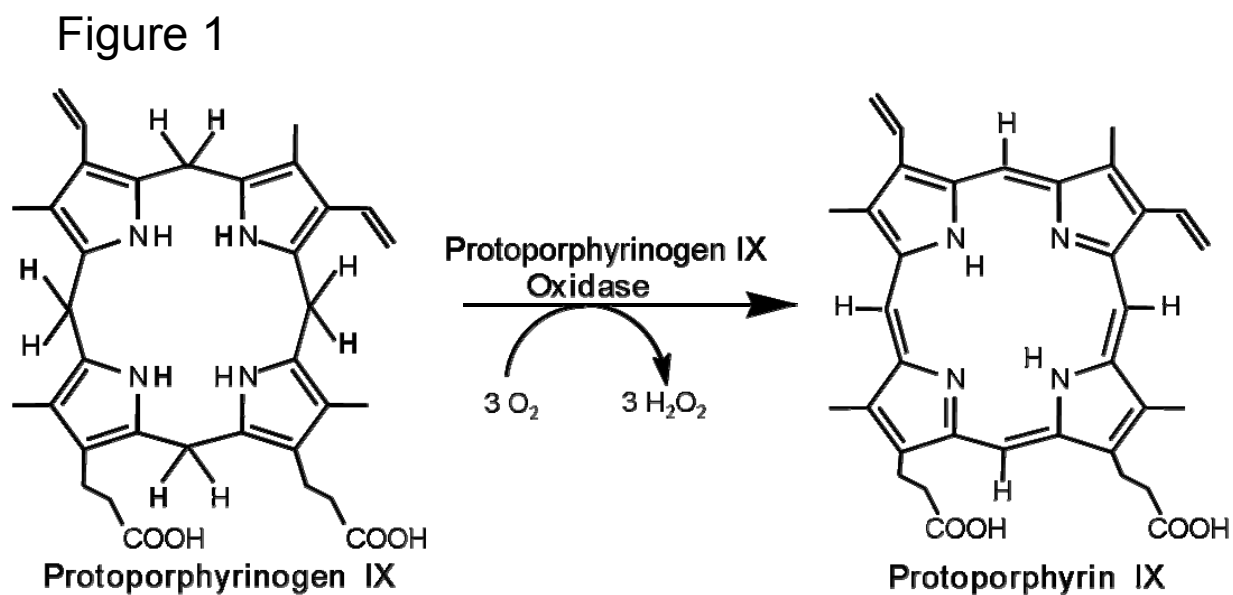


Figure 2

